



Experiment Report Form

The double page inside this form is to be filled in by all users or groups of users who have had access to beam time for measurements at the ESRF.

Once completed, the report should be submitted electronically to the User Office via the User Portal:

<https://www.esrf.fr/misapps/SMISWebClient/protected/welcome.do>

Reports supporting requests for additional beam time

Reports can be submitted independently of new proposals – it is necessary simply to indicate the number of the report(s) supporting a new proposal on the proposal form.

The Review Committees reserve the right to reject new proposals from groups who have not reported on the use of beam time allocated previously.

Reports on experiments relating to long term projects

Proposers awarded beam time for a long term project are required to submit an interim report at the end of each year, irrespective of the number of shifts of beam time they have used.

Published papers

All users must give proper credit to ESRF staff members and proper mention to ESRF facilities which were essential for the results described in any ensuing publication. Further, they are obliged to send to the Joint ESRF/ ILL library the complete reference and the abstract of all papers appearing in print, and resulting from the use of the ESRF.

Should you wish to make more general comments on the experiment, please note them on the User Evaluation Form, and send both the Report and the Evaluation Form to the User Office.

Deadlines for submission of Experimental Reports

- 1st March for experiments carried out up until June of the previous year;
- 1st September for experiments carried out up until January of the same year.

Instructions for preparing your Report

- fill in a separate form for each project or series of measurements.
- type your report, in English.
- include the reference number of the proposal to which the report refers.
- make sure that the text, tables and figures fit into the space available.
- if your work is published or is in press, you may prefer to paste in the abstract, and add full reference details. If the abstract is in a language other than English, please include an English translation.



	Experiment title: Formation of active Pd species in UiO-67 metal organic framework for catalytic hydrogenation of carbon dioxide	Experiment number: CH-5983
Beamline: BM31	Date of experiment: from: 01.04.2021 to: 06.04.2021	Date of report: 24.01.2022
Shifts: 18	Local contact(s): Dragos Stoian (email: dragos.stoian@esrf.fr)	<i>Received at ESRF:</i>
Names and affiliations of applicants (* indicates experimentalists, **remote access): Oleg A. Usoltsev ^{1**} , Aram L. Bugaev ^{1**} , Alina Skorynina ^{1**} , Elizaveta Kozyr ^{1,2**} , Anna Pnevskaya ^{1**} , Dragos Stoian ^{2*} ¹ Southern Federal University, Rostov-on-Don, Russia ² University of Turin, Turin, Italy ³ ESRF, Grenoble, France		

Report:

An interplay between metal and oxide phases of palladium as well as their spatial distribution in the volume of palladium particles are important parameters relevant for numerous catalytic reactions. By applying in situ time-resolved X-ray absorption spectroscopy we have provided a solid proof of a core-shell structure formed in the 3 nm palladium nanoparticles upon exposure to molecular oxygen. Detailed analysis of X-ray absorption spectra revealed the restructuring of the fcc-like palladium surface into the 4-coordinated structure of palladium oxide upon absorption of oxygen from the gas phase. Comprehensive analysis of spectral data gives an unambiguous proof of oxidic shell/metallic core structure formed upon oxidation. The metallic core is preserved in the 50-200 °C range even after continuous exposure to oxygen, with its size increasing insignificantly upon increasing the temperature. Above 200 °C, the particles get fully oxidized, the kinetics and saturated values being strongly dependent on the temperature. Finally, the effect of water formed under reaction conditions and the particle size effect are also discussed. The suggested methodology can be further extended for unambiguous discrimination of bulk and surface palladium oxides under reaction conditions. The draft of the manuscript is ready and will be submitted in February-March 2022.

Overview of the main results:

During the experimental procedure, the reduced Pd(0) particles were exposed to 20% O₂/He feed with continuous collection of XAS data. The procedure was repeated for selected temperatures in 50 – 400 °C range. The PCA analysis revealed only two components in the whole XANES dataset except for the data collected at 50 °C. The additional component observed when adding the latter set of data was related to the formation of palladium hydride. Therefore the further MCR analysis was performed using only two components, representing Pd(0) metallic phase, and Pd(II) oxide (See Figure S1). The results of MCR analysis for all studied temperatures are summarized in Figure 1. Below 200 °C, a rapid increase of Pd(II) fraction is observed as soon as O₂ is present in the feed followed by a slower process visible over an hour time-scale. The saturated value of Pd(II) fraction increases from ca. 0.3 to ca. 0.5

for the temperatures increasing from 50 to 180 °C. Starting from 220 °C another behavior is observed, resulting in further grows of Pd(II) with kinetics strongly dependent on temperature. The saturated values of Pd(II) fraction are summarized in Figure S2. Considering the 3 nm size of the particles, which have about 30% of surface atoms, the rapid growth of Pd(II) fraction at the beginning of each oxidation procedure can be explained by the surface oxidation.

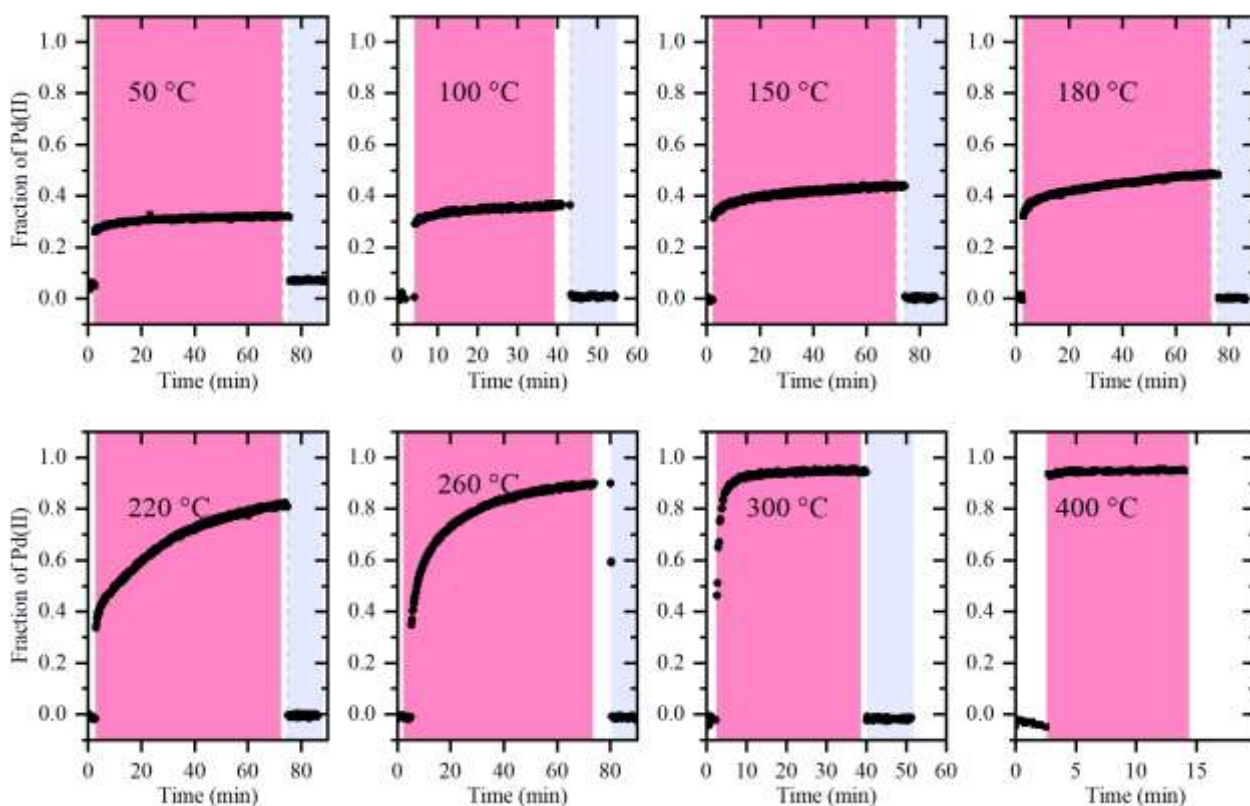


Figure 1. Results of MCR analysis of XANES for Pd/Al₂O₃ during oxidation (red background) and reduction (blue background) at different temperatures. White background corresponds to inert atmosphere.

To prove the above hypothesis the following analysis of EXAFS was performed. At the first stage, we have compared the Fourier-transformed (FT) spectrum of Pd/Al₂O₃ (Figure S3). Notably, the first shell Pd–O contribution (1 – 2 Å region, phase-uncorrected) is similar in both samples, while the Pd–Pd contribution (3 Å, phase-uncorrected) is significantly reduced in the catalyst due to the nanometric dimensions of the NPs. The latter means, that all Pd atoms in the NPs, including the surface ones, are 4-coordinated with oxygen, making the first-shell Pd–O peak independent on the particle size, which was also confirmed numerically by first-shell fit. The next fact, demonstrated in Figure S4, is that even for the temperatures below 200 °C, when only surface oxidation was hypothesized, not only the growth of first shell Pd–O is observed in FT-EXAFS data, but also a decrease of metallic Pd–Pd contribution. This indicates that upon adsorption of oxygen the restructuring of the surface layer from fcc-like 12-coordinated structure of Pd(0) into the 4-coordinated structure of PdO occurs.

The above structural observations were implemented in the following model for EXAFS fitting: (i) the fit was performed with two contributions, Pd–O and Pd–Pd with relative fractions of α and $(1 - \alpha)$, respectively; (ii) interatomic distances, zero energy shift and Debye-Waller parameter were independently varied for each contribution; (iii) coordination number for Pd–Pd was varied, while for Pd–O it was fixed to 4. This model neglects the second coordination shell (Pd–Pd) of the oxide phase, but this contribution is first of all much weaker than Pd–Pd contribution from metal (e.g. compare the intensities of FT-EXAFS in Figure S3, red, and S4, black) and also in this *in situ* experiment the high fractions of oxides are observed for high

temperatures, where Pd–Pd contribution is significantly suppressed (Figure S5). Finally, the Pd–Pd contribution of the oxide phase is located in higher R -region comparing to the metal (3.0 vs 2.5 Å, phase-uncorrected).

In such a way, the fraction of oxide phase, α , was obtained from fitting the time-resolved EXAFS data (Figure 2). The behavior and numerical values of α are in good agreement with Pd(II) fraction from XANES (Figure 1). The reduction parts were not analyzed, since in absence of the oxide fraction, the inclusion of Pd–O contribution led to unreasonable values associated with this path. At the same time, to reduce the correlations between variable parameters by using a longer k -range, the fit was also performed on the spectra averaged over the last 3 minutes of each oxidation procedure (Table 1). The remarkable is the decrease of coordination numbers associated with the Pd–Pd path of the metallic palladium phase, which correlates with the fact that upon increasing of the PdO shell, the size of the metallic core decreases. It should be also noted that the values of α , reported in Table 1 are the same as those, obtained from the time-resolved data.

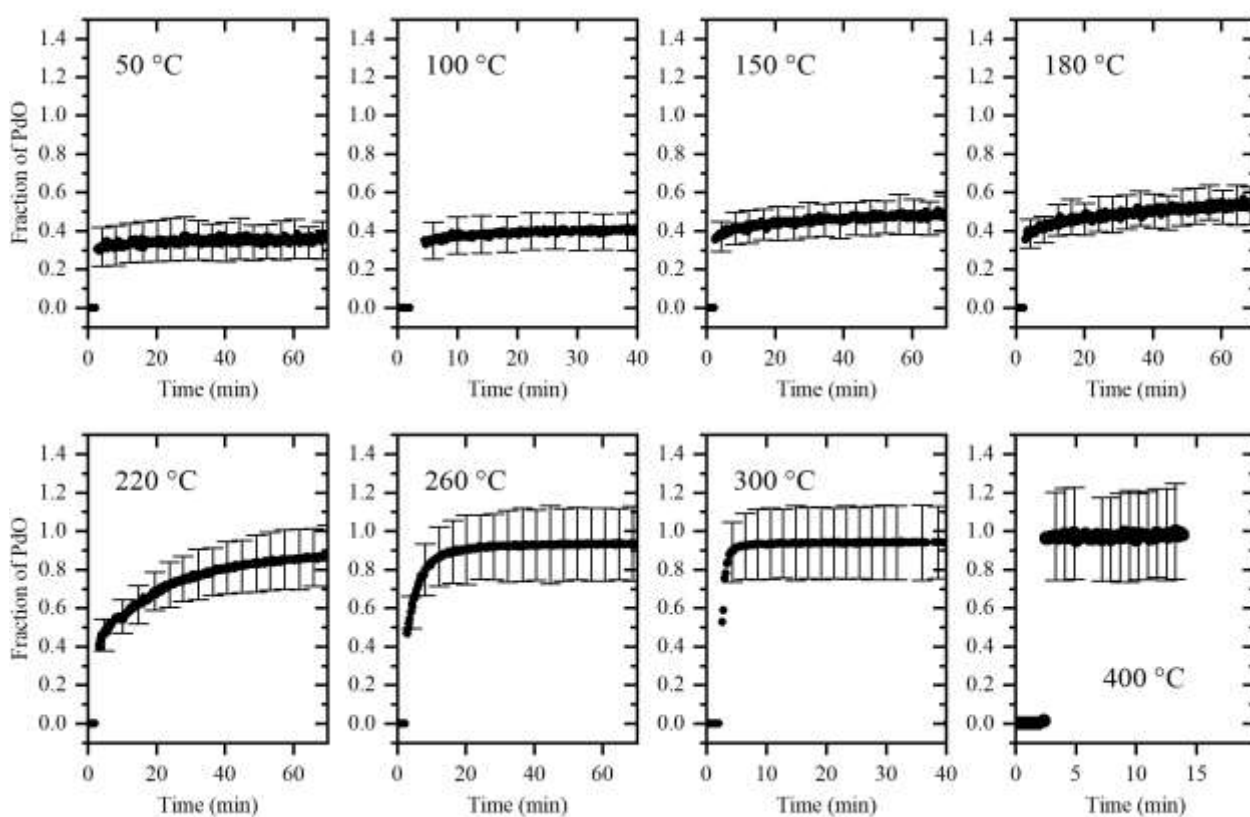


Figure 2. Fraction of PdO phase, α , obtained by fitting the time-resolved EXAFS data for Pd/Al₂O₃ during oxidation at different temperatures.

Table 1. Structural parameters for Pd–Pd shell of the metallic palladium phase remaining after oxidation at different temperatures and the fraction, α , of PdO phase. The values were obtained by fitting the averaged spectra.

T , °C	R , Å	N	σ^2 , Å ²	$1 - \alpha$
50	2.73	± 9.5	± 0.008	± 0.38
	0.01	0.8	0.001	0.05
100	2.73	± 9.1	± 0.009	± 0.42
	0.01	0.9	0.001	0.05
150	2.72	± 8.7	± 0.010	± 0.49
	0.01	1.1	0.001	0.05
220	2.71	± 6.1	± 0.009	± 0.83
	0.02	2.1	0.003	0.08

The size effect was also investigated by measuring Pd/P4VP sample with particle size of ca. 1 nm (Figures S8-9). In agreement with the particle size, the fraction of PdO phase, attributed to the surface oxide, is higher already at room temperature in both XANES and EXAFS data, due to higher surface-to-bulk ratio. The temperature range for this sample was limited, since above 180 °C the particles sinter and reduce to Pd(0). A similar effect was observed earlier for this type of sample in the process of alcohol oxidation.